Applied Thermal Engineering 132 (2018) 545–553

Contents lists available at ScienceDirect

Applied Thermal Engineering

journal homepage: www.elsevier.com/locate/apthermeng

Research Paper

Thermodynamic and economic analysis of zeotropic mixtures as working fluids in low temperature organic Rankine cycles

Bensi Dong [a], Guoqiang Xu [a], Tingting Li [b], Yongkai Quan [a], Jie Wen [a,*]

[a] National Key Laboratory of Science and Technology on Aero-thermodynamics, School of Energy and Power Engineering, Beihang University, Beijing 100191, China
[b] Department of Mechanical Engineering, Texas A&M University, College Station, TX 77843-3123, United States

HIGHLIGHTS

- Higher net power output by using zeotropic mixtures is achieved at the cost of larger heat transfer area.
- Pure ORC shows more net power than zeotropic ORC under the same heat exchanger area.
- Power demand and pinch point temperature are the basis for selecting pure ORC or zeotropic ORC.

ARTICLE INFO

Article history:
Received 31 July 2017
Revised 18 December 2017
Accepted 23 December 2017
Available online 28 December 2017

Keywords:
Organic Rankine cycle
Zeotropic mixtures
Refrigerant
Pinch analysis
Economic performance

ABSTRACT

Organic Rankine cycle (ORC) is one of the most technically feasible methods to convert low-grade thermal energy into shaft power. An efficient approach to improve the thermodynamic performance is using zeotropic mixtures that enables better temperature match with the heat source and sink. In this article, a thorough assessment of thermodynamic and economic performance is conducted for the low grade ORCs using pure fluid and zeotropic mixtures. This work also examines the effects of heat source temperature and mixture mass fraction on the net power output, heat exchanger size, and cost-effective performance, and discusses the according basis for the selecting pure fluid or zeotropic mixtures. The results show that zeotropic ORC is capable of producing more net power than pure ORC, particularly for heat source with larger temperature difference. However, it needs much more heat exchanger area and therefore causes an unfavorable economic performance. Under the same heat exchanger area, pure cycle has lower pinch point temperature and higher net power output than zeotropic cycle. Therefore, the selection between pure fluid and zeotropic mixtures is also dependent on whether the power demand can be satisfied in pure ORC under the given pinch point condition.

1. Introduction

With human energy demand increasing over 40% since 2000 [1], the associated worldwide energy crisis and environment problems have been forcing people to develop energy-saving solutions and alternative energy sources. Low-grade heat from renewable thermal energy/waste heat is one of the prevailing research subjects due to its abundance and environmental friendliness. In the framework of converting low-grade thermal energy into electricity, organic Rankine cycle (ORC) is proposed as a promising method due to its high efficiency and reliability, small size, and low emission [2]. The ORC principle is similar to the steam Rankine cycle but using organic substance with low boiling temperature as working fluid. Therefore, the selection of working fluid is one of the most concerns in ORC research. A broad range of pure working fluid candidates have been investigated. In general, R123 [3], R134a [4], R245fa [5], and N-pentane [6] are typically selected as the working fluids of middle-low temperature ORC due to their outstanding comprehensive properties. Besides, toluene [7] and siloxanes [8] with good thermal stability are more suitable for high-temperature ORC.

With the in-depth research, the ORC using pure fluid (pure ORC) has been recognized to be substantially potential. To further improve the cycle performance, ORC using zeotropic mixtures (zeotropic ORC) as working fluid was proposed. Due to the non-isothermal property during the phase change process, zeotropic mixtures can match better with the temperature in the heat source or sink, leading to a smaller exergy destruction and therefore a better thermodynamic performance. Zeotropic mixtures has been widely used in the refrigeration cycles to improve the cooling performance [9]. The first Rankine cycle employing zeotropic mixtures

* Corresponding author.
E-mail address: wenjie@buaa.edu.cn (J. Wen).

https://doi.org/10.1016/j.applthermaleng.2017.12.083
1359-4311/

Nomenclature

M	molar mass [kg/kmol]
P	pressure [kPa]
T	temperature [°C]
Q	heat absorption capacity [kW] or heat flux [W/m2]
W	power output [kW]
m/G	mass flow rate [kg/s]
h	specific enthalpy [kJ/kg]
d/D	diameter [m]
Re	Reynolds number
Pr	Prandt number
Pr	reduced pressure [kPa]
x	vapor quality
Cs	liquid heat capacity [J/(kg °C)]
y	mole fraction
n	total number of components

Greek symbols

η	cycle efficiency [%] or viscosity [Pa·s]
λ	thermal conductivity [W/(m °C)]
ρ	density [kg/m3]

Subscripts

evap	evaporation
cond	condensation
source	heat source
sink	heat sink
gen	power generation
out	heat source outlet
v	vapor
l	liquid
d	dew point
b	bubble point
vp	vaporization
s	saturation

is Kalina cycle [10], where the working fluid is typically ammonia and water but the mixing state of ammonia and water only exists in the heat transfer processes.

The research of zeotropic ORC began in the 1990s due to the establishment and development of the properties prediction models for fluid mixtures. Angelino et al. [11] firstly evaluated the merits of organic-fluid mixtures as the working fluids of ORCs for heat recovery and geothermal applications, and found no efficiency increase in the zeotropic ORC comparing to pure ORC. Similar conclusions are documented in the studies of Wang et al. [12] and Li et al. [13]. However, their findings are limited to the operating conditions [14]. Chys et al. [15] analyzed the effect of using mixtures in ORC through pinch analysis method and provided the method to determine the optimal zeotropic mixtures. The results showed that the use of zeotropic mixtures has positive effect on the ORC performance, and the cycle efficiency increases up to 20% for the low temperature heat source.

Many existing studies also adopted pinch analysis method to evaluate the performance of zeotropic ORC. Dong et al. [2] analyzed the performances of zeotropic mixtures MM/MDM as working fluid for high temperature ORC. The results indicated that the zeotropic mixture leads to a cycle efficiency increase compared to pure fluid and condensation parameters affect the cycle efficiency more significantly than evaporation conditions. Liu et al. [16] discussed the effects of the condensation temperature glide of the zeotropic mixtures on the cycle performance and stated that zeotropic ORC has better thermodynamic performance when the condensation temperature glide is close to the cooling water temperature increase. According to Zhao and Bao [17], heat source inlet temperature has significant influence on the optimal composition of zeotropic mixtures, and there exists a heat source inlet temperature with no high efficiency advantage for zeotropic ORC. Heberle et al. [18] presented the simulations of zeotropic ORCs for low-grade geothermal resources and their results showed that the second law efficiency can be increased by adding a less volatile component in a mixture for higher heat source temperature. Chen et al. [19] proposed a concept of zeotropic transcritical ORC and the efficiencies of the ORCs with R134a/R32 is 10–30% higher than the cycles using R134a. Li et al. [13] evaluated the effects of internal heat exchanger on pure and zeotropic ORCs and proposed that the increase of thermal and exergy efficiencies by adding a recuperator is higher for R141b/RC318 than pure R141b. Sadeghi et al. [20] thoroughly investigated the performance of various ORC configurations using zeotropic mixtures. It was found that using zeotropic mixtures improves the power generation in different configurations. The series of two-stage evaporator ORC using R407A as working fluid has the highest net power output. Wu et al. [21] explored the economic performance of zeotropic mixtures for ORC based on the net power output per unit UA (the product of heat transfer coefficient and heat transfer area). However, the results indicated the economic performance becomes worse compared to that of pure ORC. The study by Zhao and Bao [22] showed that composition shift on zeotropic ORC significantly lowers the net output work and the thermal efficiency. In addition to the thermodynamic analysis and modeling, several experimental investigation relating to zeotropic ORC also have been performed [23–25].

By far, pinch analysis is the most widely used method to analyze zeotropic ORC. Multiple evaluation indexes, e.g. cycle efficiency, exergy efficiency, and net power output, have been selected to compare the thermodynamic performances between pure cycle and zeotropic cycle. However, to the best of our knowledge, the analysis in zeotropic ORC is rarely performed by accounting for the heat exchanger area. It is necessary to further study the economic performance of zeotropic ORC for the following reasons: (1) Non-isothermal behavior of zeotropic mixtures may lead to a smaller heat transfer temperature difference under the same pinch point temperature; (2) Due to the mass transfer resistance, the heat transfer coefficient of zeotropic mixtures in the phase transition step is smaller than that of pure constitutive fluids [26]. These factors can both affect the demand for heat transfer area and therefore the economic performance.

To fill the shortcoming in the existing literature, this study explores the thermodynamic and economic performance of the low-temperature ORC using refrigerants and their mixtures. A thermodynamic and heat transfer coupling model is developed to investigate the effects of heat source temperature and mixture mass fraction on the net power output, heat exchanger size, and cost-effective performance. According to the results, the guidance for the selecting pure fluid or zeotropic mixtures is proposed at last.

The paper starts with the introduction section followed by Section 2 which describes the cycle and considered working fluids. Then, Section 3 gives the method of simulation in this work. The

results and discussion are presented in Section 4, including the thermodynamic performance, economic performance, and the comparison between pure and zeotropic ORCs. Lastly, Section 5 draws the research conclusions and provides the related research prospects.

2. ORC and working fluids

The schematic and temperature–entropy curve of the zeotropic ORC are shown in Fig. 1. The basic ORC includes an expander to generate shaft power output, a condenser to condense the working fluid, a pump to elevate the cycle pressure and an evaporator to absorb heat from the heat source. In the condenser and evaporator, the variable temperature of the zeotropic mixtures during the phase transition process could improve the temperature match between the working fluid and the heat transfer medium. Besides, variable temperatures can also widen the average temperature difference between evaporation and condensation processes. Both of them help improve the thermodynamic performance of the cycle.

The conditions of the heat source, heat sink and ORC process parameters are summarized in Table 1. Both the heat source and heat sink media are water at different pressures. The heat source outlet temperature is varied to investigate its influence on the cycle performances, while other parameters are constant and mainly obtained from Chys et al. [15]. Among them, the pinch point temperature in the condenser is lower than that in the evaporator due to its relatively significant effect on the cycle efficiency [2].

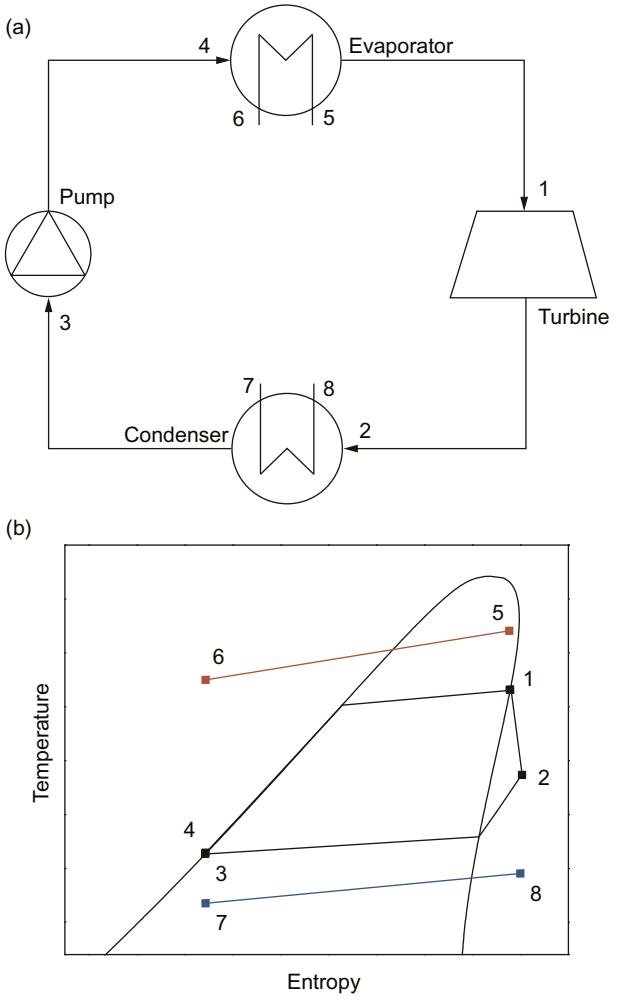

Fig. 1. (a) Schematic and (b) T-s curves of zeotropic ORC.

Table 1
Parameters for the heat source, heat sink and cycle.

Heat source (water)	Inlet temperature	150 °C
	Pressure	500 kPa
	Mass flow rate	25 kg/s
Heat sink (water)	Inlet temperature	25 °C
	Outlet temperature	35 °C
	Pressure	150 kPa
ORC	Isentropic pump efficiency	80%
	Isentropic turbine efficiency	75%
	Pinch temperature in the evaporator	20 °C
	Pinch temperature in the condenser	10 °C

Working fluid selection is fundamental in ORC design. Each component in the mixture fluids is required to satisfy the chemically stability requirement and exhibit the suitable thermal properties. Due to the condition of the heat source temperature and the limits of the adopted heat transfer models, refrigerants are selected as the potential components. Since the ORC in this work is a subcritical cycle with the saturated vapor at the turbine inlet, only dry fluids or isentropic fluids (the slope of the saturated vapor line in the T-s diagram is infinite or positive) are considered. The critical temperature of the fluid candidate should be higher than 150 °C based on the heat source temperature, while its boiling temperature should not be significantly higher than the heat sink temperature to avoid extremely low condensation pressure. By following these guidelines, five commonly used ORC working fluids, R245fa, R245ca, R123, R365mfc, and R113, are selected as the candidates. Their main thermal properties and the saturation curves of R123, R365mfc, and R123/R365mfc (0.5/0.5) are given in Table 2 and Fig. 2, which are derived from the fluid property database REFPROP 9.0 [27].

3. Simulation method

An original Matlab program is developed to simulate the described cycle with various working fluids. The simulation is evaluated under the assumptions that the cycle operates at steady state, pressure drop and heat loss through the pipes and heat exchangers are neglected, and the composition shaft of the zeotropic mixtures is not considered.

The modeling process applies the pinch analysis method and its flow chart is shown in Fig. 3, where the subscripts 1 and 3 are the state points in Fig. 1. The temperature profile of the cycle is determined by the conditions of the heat source and sink, offset by pinch point temperatures. The turbine inlet temperature T_1 and the condenser outlet temperature T_3 are determined by the pinch point temperatures in the evaporator and condenser, respectively. The energy balance in each component of the cycle can be calculated by:

$$Q_x - W_x = m(h_j - h_i) \tag{1}$$

where Q, W, m, and h represent the heat absorption capacity, power output, mass flow rate, and specific enthalpy, respectively. The subscripts i and j are the inlet and outlet of the component x.

To determine the pinch point temperature, the temperature profile of the mixture in the phase change process is divided into 30 segments based on the same temperature step. Then the temperature of water in each corresponding segment can be calculated by the energy conservation equation. The pinch point temperature can be therefore obtained by:

$$T_{pinch.evap} = \min\{T_{source}(i) - T_{evap}(i)\}, i = 1, 2 \ldots 30 \tag{2}$$

$$T_{pinch.cond} = min\{T_{cond}(i) - T_{sink}(i)\}, i = 1, 2 \ldots 30 \tag{3}$$

Table 2
Fluid properties of the selected refrigerants.

Fluid	M [g/mol]	$P_{critical}$ [kPa]	$T_{critical}$ [°C]	$T_{boiling}$ [°C]
R245fa	134.05	3651	154.01	15.14
R245ca	134.05	3925	174.42	25.13
R123	152.93	3662	183.68	27.82
R365mfc	148.07	3266	186.85	40.15
R113	187.38	3392	214.06	47.59

M: molar mass; $P_{critical}$: critical pressure; $T_{critical}$: critical temperature; $T_{boiling}$: boiling temperature.

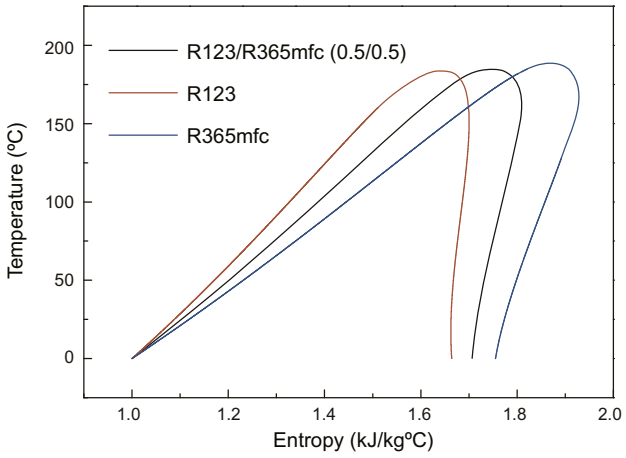

Fig. 2. Saturated curves of R123, R365mfc, and R123/R365mfc (0.5/0.5).

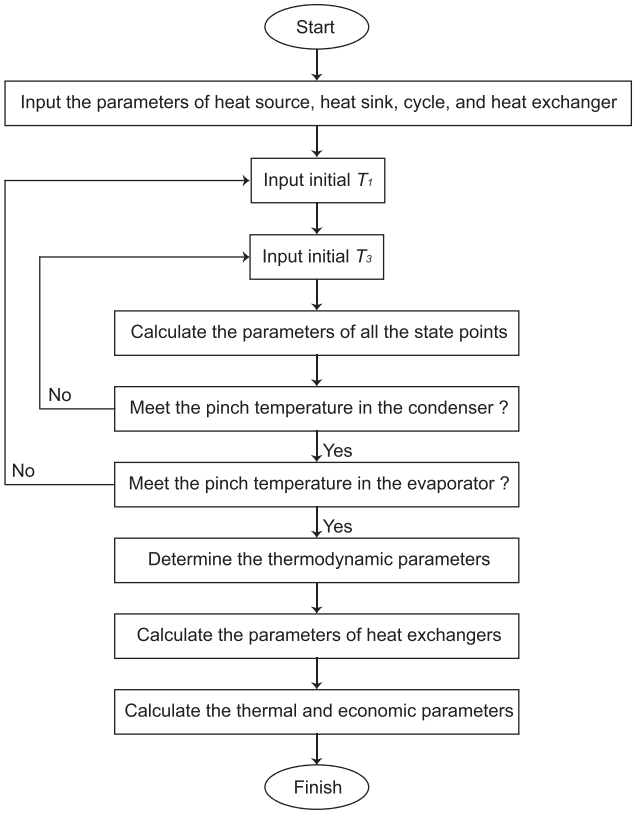

Fig. 3. The flow chart of the simulation.

where the subscripts *source* and *sink* represent the heat source and the heat sink. After these initial input parameters being updated to meet the pinch point conditions, the cycle thermodynamic parameters can be determined through Eq. (1).

As shown in Fig. 4, the concentric double pipe heat exchanger with the same size is selected as the evaporator and condenser. The heat transfer correlations used in this modeling are detailed in the Appendix A. Among them, Gnielinski and Dittus-Boelter correlations are used to calculate the single-phase heat transfer coefficients. Other correlations, developed and summarized by Bivens and Yokozeki [28], are applied to determine the evaporation and condensation heat transfer coefficients of the refrigerant flow in tubes. Based on the heat transfer coefficient in each stage together with the corresponding heat transfer capacity and mean logarithmic temperature difference, the heat exchanger area can be obtained by heat transfer equation.

In this work, the heat source is the waste heat or geothermal energy with a fixed inlet temperature, thus the design object is to get more shaft power instead of higher cycle efficiency. The net power output, which is defined as the difference between the output of the turbine and the input of the pump, is employed to evaluate the thermodynamic performance. In the economic analysis, the ratio of the net power output to the total heat exchanger area is selected as the evaluation indicator (hereinafter referred to as cost-effective performance).

The simulation method is validated with the results of the ORCs using R245fa, R365mfc and their mixtures R245fa/R365mfc (0.3/0.7) in Chys et al. [15]. As shown in Table 3, the comparisons show the results coincide within the maximum difference of 2.29%, indicating the reliability of the simulation in the present work.

4. Results and discussion

The thermodynamic performance of zeotropic ORC, which is evaluated by the net power output, is presented in the first subsection. The economic performance considering the heat exchanger area is then analyzed in the second subsection. With the above analysis, the comparison between pure cycle and zeotropic cycle is discussed in the third subsection.

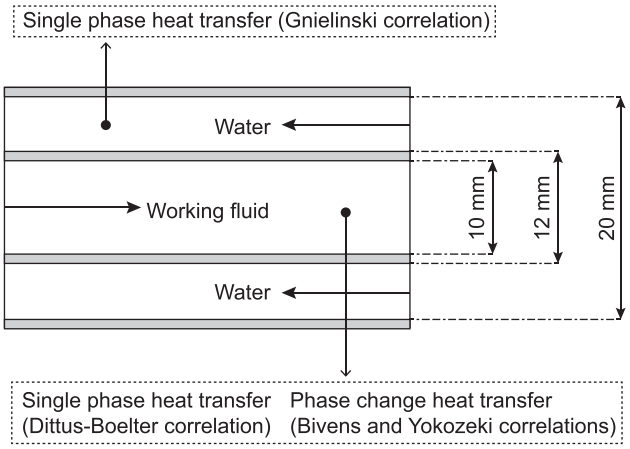

Fig. 4. The structure size of the concentric double pipe heat exchanger.

Table 3
Validation of the proposed simulation method.

	R245fa		R365mfc		R245fa/R365mfc	
	Chys	This work	Chys	This work	Chys	This work
P_{evap} [kPa]	2030	2030	940	940	1310	1340
P_{cond} [kPa]	290	290	120	120	150	150
P_{ratio}	7.1	7.1	8.1	8.1	8.7	8.7
m [kg/s]	4.47	4.46	4.25	4.25	4.28	4.28
W_{pump} [kW]	7.5	7.5	3.6	3.6	5.0	5.1
W_{gen} [kW]	100.3	100.3	104.1	104.0	109.5	109.6
η [%]	9.61	9.61	10.4	10.4	10.82	10.82

P_{evap}: evaporation pressure; P_{cond}: condensation pressure; P_{ratio}: pressure ratio; m: mass flow rate; W_{pump}: power consumed by the pump; W_{gen}: power generation; η: cycle efficiency.

4.1. Thermodynamic performance

ORC with zeotropic mixture as working fluid shows higher net power output than that using pure fluid. As illustrated in Fig. 5, the zeotropic cycle using R245fa/R113 (0.4/0.6) produces the most net power under the conditions of variable heat source outlet temperature. The advantage of using zeotropic mixture is more significant when lowering the heat source outlet temperature. For example, the mixture R245fa/R113 shows the highest net power of 251.39 kW at the outlet temperature of 130 °C, representing an increase of 2.56% for R245fa and 7.16% for R113, respectively. When the outlet temperature is 90 °C, the net power is up to 557.68 kW and the increases are 20.46% for R245fa and 14.14% for R113.

With the decrease of heat source outlet temperature, on the one hand, the cycle heat absorption increases accordingly, while on the other hand, the reduced average evaporation temperature leads to a lower cycle efficiency. Therefore, the increase of net power output by using zeotropic mixtures gets gradually smaller in the range of low heat source outlet temperature. The net power output from the cycle using R113 even decreases slightly when the heat source outlet temperature changes from 100 to 90 °C. We can also find that the net power of the cycle using R245fa/R113 fluctuates when the mass fraction of R245fa is within 0.1–0.3. Fig. 6(a) shows that when R245fa fraction is 0.2, the condensation temperature glide is 13.13 °C that is higher than the temperature difference of the cooling water. As shown in Fig. 6(b), it causes the pinch point in the condenser occurs at its outlet and therefore the average condensation temperature increases, which results in a negative impact on the net power output. Since the pinch point in the evaporator occurs at the saturated liquid state, the relatively higher evaporation temperature glide leads to a higher average evaporation temperature. The combined effects of evaporation and condensation temperatures result in the fluctuation of the net power output. It indicates that higher temperature glide does not always result in more net power output for zeotropic ORC.

Fig. 7 summarized the optimum working fluid and the maximum net power output under the different heat source outlet temperature. R245ca/R113 is more suitable for the heat source outlet

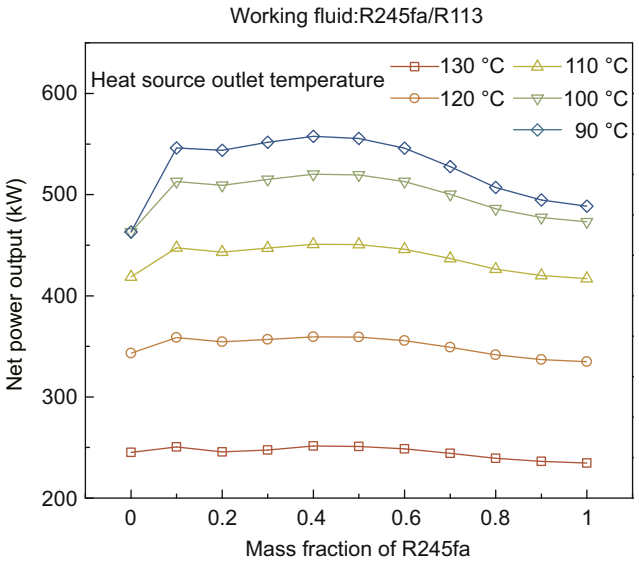

Fig. 5. Net power output versus mass fraction in the ORC using R245fa/R113.

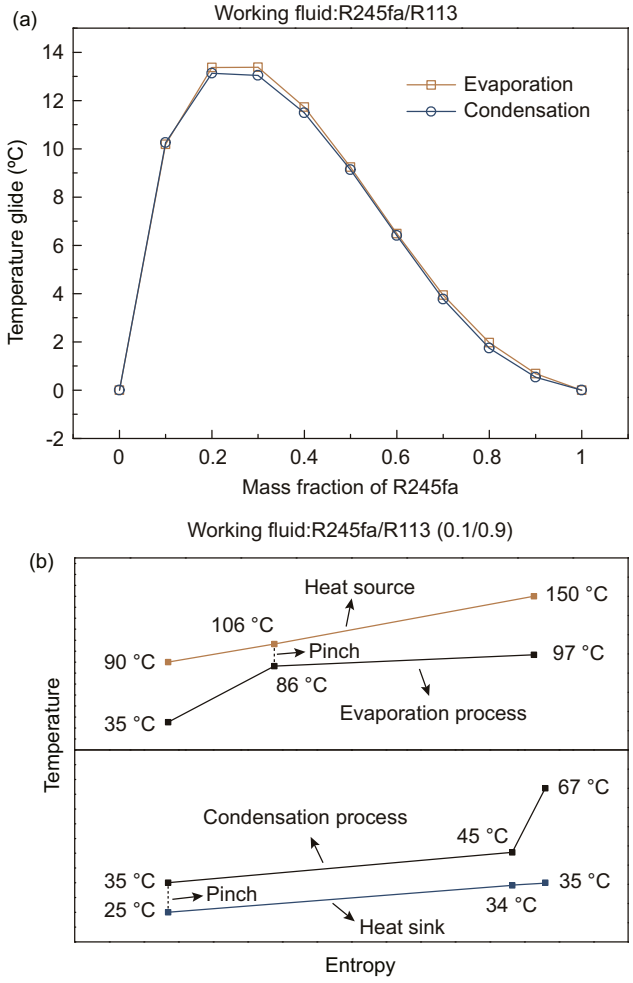

Fig. 6. (a) Temperature glide versus mass fraction in the cycle using R245fa/R113 and (b) T-s curves of the evaporation and condensation processes in the cycle using R245fa/R113 (0.1/0.9).

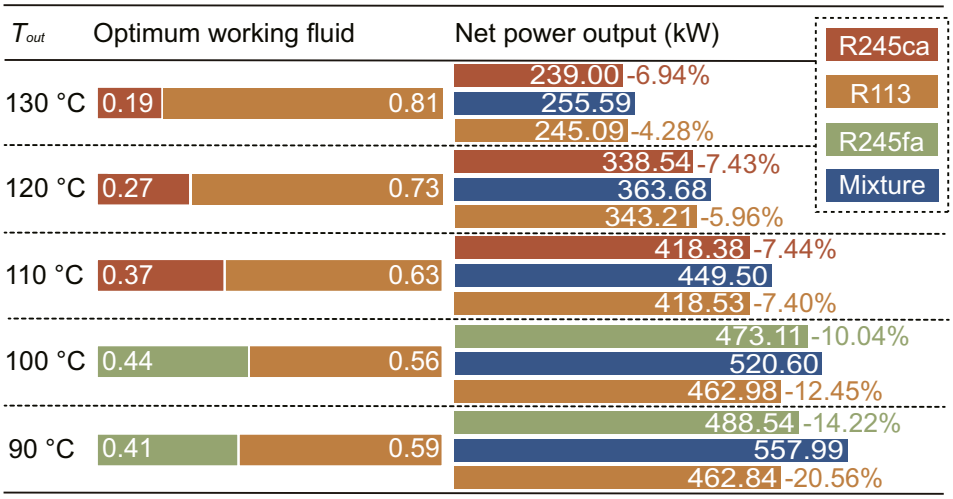

Fig. 7. The optimum working fluid and the most net power output under different heat source outlet temperature (T_{out}).

temperature in the range of 110–130 °C, and the optimum mass fraction of R245ca increases from 0.19 to 0.37 with the decrease of heat source outlet temperature. When the outlet temperature is lower than 110 °C, using R245fa/R113 shows higher net power output. Consistent with above analysis, the maximum output power increases when the heat source outlet temperature is reduced, but the increasing rate decreases gradually. However, compared with the pure cycle with relatively high power output, the rise in the output power by using mixture increases from 4.28% to 14.22% along with the decreasing heat source outlet temperature.

4.2. Economic performance

The economic analysis in this work focuses on the heat exchanger area, which is a common economic indicator in the related research [29,30]. Fig. 8 first shows the evaporation and condensation heat transfer coefficients of R245fa, R113, and their mixture with a ratio of 0.44/0.56 at the heat source outlet temperature of 100 °C. The heat transfer coefficients in the evaporation and condensation processes increase with the increase of vapor quality, but the change for R245fa/R113 is smaller. Also, the heat transfer coefficients of the mixture are lower than that of the components, especially for the evaporation process. The average evaporation heat transfer coefficient of the mixture is 8.44 kW/(m^2 °C), which is only 21.31% and 19.55% of that for R245fa and R113. By comparison, the heat transfer coefficient in the condensation process is relatively low, and the average condensation heat transfer coefficient of R245fa/R113 shows a decrease of 30.74% and 35.82% for the heat transfer coefficients of R245fa and R113.

The heat transfer areas of the evaporator and condenser can be determined based on the heat transfer capacity, the mean logarithmic temperature difference, and the heat transfer coefficient

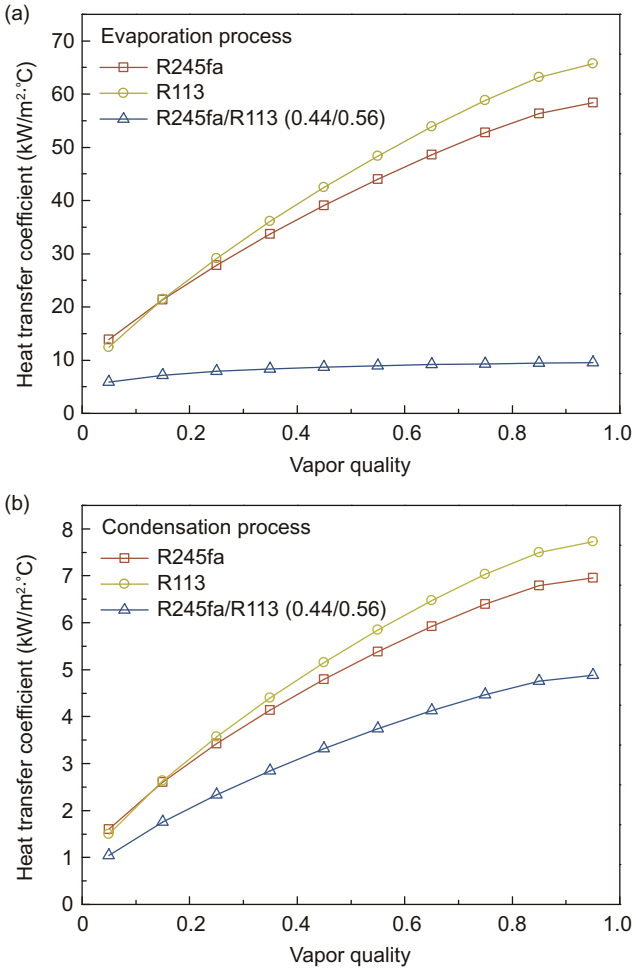

Fig. 8. Heat transfer coefficients of R245fa, R365mfc, and their mixture (0.44/0.56) along (a) evaporation process and (b) condensation process.

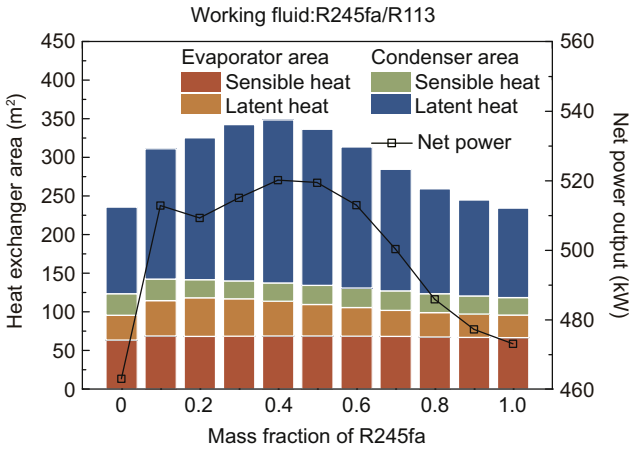

Fig. 9. Heat exchanger area versus mass fraction in the ORC using R245fa/R113.

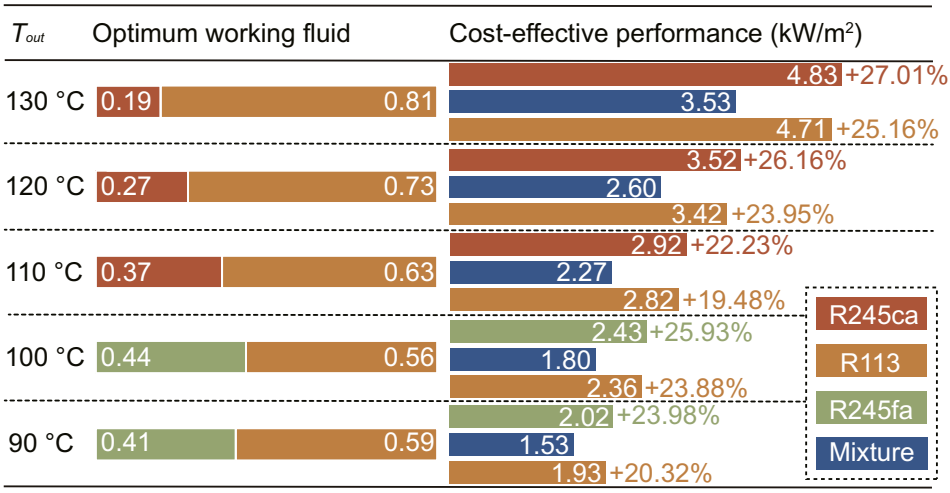

Fig. 10. Cost-effective performance of the cycle using optimum working fluid under different heat source outlet temperature (T_{out}).

obtained from the thermodynamics and heat transfer equations. Fig. 9 shows the required heat exchanger area for the cycle using R245fa/R113 at the heat source outlet temperature of 100 °C. The total heat exchanger area initially increases and then decreases with the increasing mass fraction of R245fa. The variations of the heat exchanger area and the net power output are basically the same. The biggest change in the heat exchanger area for various mass fractions appears in the latent heat stage of the condenser. The cycle using R245fa/R113 (0.4/0.6) produces the most net power of 520.17 kW and at the same time demands the largest heat exchanger area of 348.30 m^2, while using pure R245fa shows the lowest net power of 463.03 kW and also the smallest heat exchanger area of 235.60 m^2.

Fig. 10 presents the cost-effective performance of the cycle using the optimum working fluid at various heat source outlet temperature. It is worthy of note that the optimum working fluid here means that it can produce the maximum net power (see Fig. 7). Besides, since the mass flux of the working fluid increases with the decrease of the heat source outlet temperature, to obtain a reasonable tube fluid Reynolds number, the mass flux of the heat source medium is divided by 100–500 according to the conditions of the heat source temperature. Therefore, the absolute values of the cost-effective performances under different heat source outlet temperatures cannot be compared. The results of the cost-effective performance are contrary to the net power output in Fig. 7. Taking the heat source outlet temperature of 100 °C as example, compared to the pure cycle with R245fa, using R245fa/R113 (0.44/0.56) can improve the net power by 10.04%, whereas the cost-effective performance is reduced by 25.93%. In the range of the test, zeotropic cycle always shows lower cost-effective performance than pure cycle. This result illustrates that the better thermodynamic performance of zeotropic ORC is achieved at the cost of larger heat exchanger area, which results in a lower cost-effective performance.

As pure cycle shows better cost-effective performance than zeotropic cycle, the effect of the heat source outlet temperature on the cost-effective performance specific to the pure cycle is illustrated in Fig. 11. Here the relative cost-effective performance refers to the value of the cost-effective performance to the maximum value among various working fluids. The results show that adopting R123 under the heat source outlet temperature higher than 110 °C gets the highest cost-effective performance, while R245ca is suitable for the lower the heat source outlet temperature (<110 °C). By contrast, the pure cycle using R113 shows a relatively low economic performance.

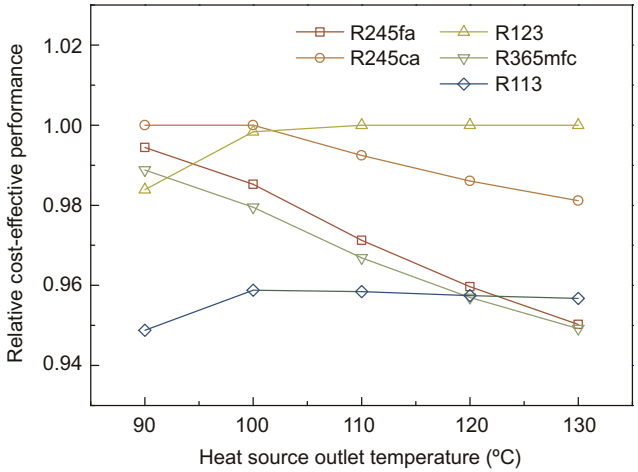

Fig. 11. Relative cost-effective performance versus heat source outlet temperature in the ORC using pure fluid.

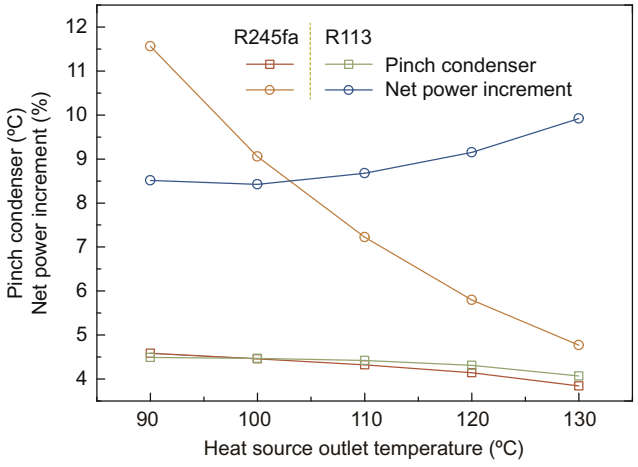

Fig. 12. Modified pinch point temperature in the condenser and net power increment for the cycle using pure fluid under the same heat exchanger area.

4.3. Comparison between pure and zeotropic ORCs

Given the above analysis, the enhancement of the net power output for zeotropic ORC is attributed to the larger heat exchanger area. Only adopting traditional pinch analysis method is not com-

Table 4
Net power increment for zeotropic ORC under the same pinch point condition.

T_{out} (°C)	Optimum fluid	Net power (kW)	Optimum mixture	Optimum ratio	Net power (kW)	Increment (%)
90	R245fa	488.54	R245fa/R113	0.41/0.59	557.99	14.22
100	R245fa	473.11	R245fa/R113	0.44/0.56	520.60	10.04
110	R113	418.53	R245ca/R113	0.37/0.63	449.50	7.40
120	R113	343.21	R245ca/R113	0.27/0.73	363.68	5.96
130	R113	245.09	R245ca/R113	0.19/0.81	255.59	4.28

prehensive enough to compare the thermodynamic performance between pure ORC and zeotropic ORC. In this section, the total heat exchanger area instead of the pinch point temperature is selected as the boundary condition. The required heat exchanger area of zeotropic ORC is obtained based on the initial pinch point condition at first, and then the result is used to model pure cycle to get a new pinch point condition and corresponding net power. Fig. 12 shows the modified pinch point temperature in the condenser and the net power increment of pure ORCs using R245fa and R113. Under the same condition of the required heat exchanger area for zeotropic cycle with R245fa/R113 (0.4/0.6), the pinch point temperature of pure ORC decreases significantly from the initial value of 10 °C to around 4 °C. Therefore, the net power output from the cycle using pure fluid is higher than using zeotropic mixture. With the decrease of the heat source outlet temperature from 130 to 90 °C, the net power increment for the cycle with R245fa increases from 4.76% to 11.56%, and the increment of using R113 decreases gradually from 9.92% to 8.51%. It tells that pure cycle can produce more power than zeotropic cycle when reducing the pinch point temperature to obtain the same heat exchanger area.

Nevertheless, when the pinch point temperature is determined, the potential of zeotropic ORC is still higher. As illustrated in Table 4, under the same pinch point condition, the net power increment by using zeotropic mixture increases from 4.28% to 14.22% with the decrease of the heat source outlet temperature from 130 to 90 °C. Therefore, power demand and pinch point temperature become the main criterion of selection pure ORC or zeotropic ORC. When the power demand is lower than the design power of pure cycle under the given minimum heat transfer temperature difference, using pure fluid shows better thermal economic performance than using zeotropic mixture. However, when the power demand exceeds the design power of using pure fluid, zeotropic ORC becomes an alternative option as it can avoid the local heat transfer deterioration.

5. Conclusion

This work investigates the thermodynamic and economic performance of the low-grade zeotropic ORC by leveraging pinch analysis method. A few of the commonly-used refrigerants, i.e. R245fa, R245ca, R123, R365mfc, R113 and their mixtures are considered as the ORC working fluids. The effects of heat source temperature and mixture mass fraction on the net power output, heat exchanger size, and cost-effective performance are investigated through a thermodynamic and heat transfer coupling model. The paper draws the main conclusions as follows:

(1) In test range, the net power output increases with the decrease of heat source outlet temperature, but the increase rate slows down gradually. Compared with pure cycle, zeotropic ORC has the capacity to produce more net power, and the net power increment is larger under a lower heat source outlet temperature.
(2) The variations of the required heat exchanger area and the net power output with the mass fraction are basically the same. Zeotropic ORC shows lower cost-effective performance than pure ORC, which indicates that higher power output is achieved at the cost of larger heat exchanger area.
(3) Under the boundary condition of the same heat exchanger area, pure cycle shows lower pinch point temperature and higher net power output than zeotropic cycle. Therefore, power demand and pinch point temperature become the basis for the selection of pure ORC or zeotropic ORC. If the power demand can be met for pure cycle under the given pinch point condition, pure fluid should be selected as the ORC working fluid. Otherwise, zeotropic ORC can yield higher output power with relatively higher pinch point for the heat exchanger.

Generally, zeotropic ORC may not always show outstanding economic performance. But it is still potential for the next generation ORC if environmental impact is required to be accounted for, because zeotropic mixtures can significantly expand the selection range of ORC working fluids. It is worthy of further researches on the heat transfer coefficient of the promising zeotropic mixtures and experiment so as to verify the conclusion in this work.

Acknowledgement

B.D. gratefully acknowledges financial support from the China Postdoctoral Science Foundation (No. 2017M620577) and the "Zhuoyue" postdoctoral program at Beihang University. The authors acknowledge the editors for handling the manuscript and the reviewers for their constructive comments that have significantly improved the manuscript.

Appendix A

For the working fluid in the outer pipe, the single-phase heat transfer coefficient is using Gnielinski equation for calculation:

$$h = \frac{\lambda}{d}\frac{(f/8)(Re-1000)Pr}{1+12.7(f/8)^{1/2}(Pr^{2/3}-1)} \tag{A.1}$$

$$f = (1.82lgRe - 1.64)^{-2}$$

For the working fluid in the inner pipe, its single-phase heat transfer coefficient is calculated by Dittus-Boelter equation:

$$h = 0.023\frac{\lambda}{d}Re^{0.8}Rr^{m} \tag{A.2}$$

with $m = 0.3$ for cooling and $m = 0.4$ for heating.

Following correlations are developed and summarized by Bivens and Yokozeki [28]. The evaporation heat transfer coefficient can be calculated as follows:

$$h = \left(A^{2.5} + B^{2.5}\right)^{1/2.5} \tag{A.3}$$

$$h = \frac{55Q^{0.67}P_r^{0.12}}{\sqrt{m}(-\lg(P_r))^{0.55}}$$

$$B = 2.838h_{lx}Fr^{0.2}(0.29 + 1/X_{tt})^{0.85}, \text{for } Fr \leqslant 0.25$$

$$B = 2.15h_{lx}(0.29 + 1/X_{tt})^{0.85}, \text{for } Fr \geqslant 0.25$$

$$Fr = \frac{(G/\rho_l)^2}{9.80665D}, X_{tt} = (1/x - 1)^{0.9}\sqrt{\rho_v/\rho_l}(\eta_l/\eta_v)^{0.1}$$

$$h_{lx} = 0.23\frac{\lambda_l}{D}Re_x^{0.8}Rr^{0.4}, Re_x = GD(1-x)/\eta_l, Pr = C_s\eta_l/\lambda_l$$

where m: molecular weight; Q: heat flux (W/m^2); P_r: reduced pressure; x: vapor quality; D: diameter (m); G: mass flux (kg/m^{2}s); λ: thermal conductivity (W/(m K)); η: viscosity (Pa s); ρ: density (kg/m^3); C_s: liquid heat capacity (J/(kg K)); subscript v: vapor; subscript l: liquid.

For mixtures:

$$h_{mix} = \frac{h_{id}}{1 + h_{id}F/Q} \tag{A.4}$$

$$F = 0.175(T_d - T_b)\left\{1 - exp\left(-\frac{Q}{1.3\times10^{-4}\rho_l H_{vp}}\right)\right\}$$

where T_d: dew point temperature (K); T_d: bubble point temperature (K); Q: heat flux (W/m^2); H_{vp}: heat of vaporization (J/kg); ρ_l: liquid density (kg/m^3).

For pure compounds, following empirical correlation for the condensation process is applied:

$$h/h_l = (1-x)^{0.8} + 3.8x^{0.76}(1-x)^{0.04}(P_c/P_s)^{0.38} \tag{A.5}$$

$$h_l = 0.023\frac{\lambda}{D}Re^{0.8}Rr^{0.4}, Re = GD/\eta, Pr = C_s\eta/\lambda, h_{con} = hF,$$
$$F = 0.78738 + 6187.89G^{-2}$$

where x: vapor quality; P_c: critical pressure; P_s: saturation pressure; D: diameter (m); G: mass flux (kg/(m^2 s)); λ: liquid thermal conductivity (kg/(m K)); η: liquid viscosity (Pa s); C_s: liquid heat capacity (J/(kg K)); h_{con}: condensation heat transfer coefficient (W/(m^2 K)).

For mixtures:

$$h_{mix} = \left\{\sum_{i=1}^{n}(y_i/h_i)^c\right\}^{-1/c} \tag{A.6}$$

$$c = 0.85 - 0.014545(T_d - T_b), \text{for } G \geqslant 160$$

$$c = (0.10676 + 0.12483ln(G))(1.25 - 0.04545(T_d - T_b)), \text{for } G \geqslant 160$$

where y_i: mole fraction of component; h_i: heat transfer coefficient (W/(m^2 K)); n: total number of components; T_d: dew point temperature (K); T_b: bubble point temperature (K).

References

[1] B. p.l.c, BP Energy Outlook, <http://www.bp.com/>, 2016.
[2] B. Dong, G. Xu, Y. Cai, H. Li, Analysis of zeotropic mixtures used in high-temperature organic Rankine cycle, Energy Convers. Manage. 84 (2014) 253–260.
[3] Z.Q. Wang, N.J. Zhou, J. Guo, X.Y. Wang, Fluid selection and parametric optimization of organic Rankine cycle using low temperature waste heat, Energy 40 (2012) 107–115.
[4] K. Darvish, M. Ehyaei, F. Atabi, M. Rosen, Selection of optimum working fluid for organic Rankine cycles by exergy and exergy-economic analyses, Sustainability 7 (2015) 15362–15383.
[5] H. Yu, X. Feng, Y. Wang, A new pinch based method for simultaneous selection of working fluid and operating conditions in an ORC (Organic Rankine Cycle) recovering waste heat, Energy 90 (2015) 36–46.
[6] A.A. Jubori, A. Daabo, R.K. Al-Dadah, S. Mahmoud, A.B. Ennil, Development of micro-scale axial and radial turbines for low-temperature heat source driven organic Rankine cycle, Energy Convers. Manage. 130 (2016) 141–155.
[7] Y. Cao, Y. Gao, Y. Zheng, Y. Dai, Optimum design and thermodynamic analysis of a gas turbine and ORC combined cycle with recuperators, Energy Convers. Manage. 116 (2016) 32–41.
[8] A.S. Panesar, An innovative organic Rankine cycle approach for high temperature applications, Energy 115 (2016).
[9] K.D. Timmerhaus, C. Rizzuto, Cryogenic Mixed Refrigerant Processes, Springer, New York, 2008.
[10] A.I. Kalina, Combined cycle and waste heat recovery power systems based on a novel thermodynamic energy cycle utilizing low-temperature heat for power generation, Mech. Eng. 105 (1983), 104–104.
[11] G. Angelino, P. Colonna di Paliano, Multicomponent working fluids for organic Rankine cycles (ORCs), Energy 23 (1998) 449–463.
[12] X.D. Wang, L. Zhao, Analysis of zeotropic mixtures used in low-temperature solar Rankine cycles for power generation, Sol. Energy 83 (2009) 605–613.
[13] W. Li, X. Feng, L.J. Yu, J. Xu, Effects of evaporating temperature and internal heat exchanger on organic Rankine cycle, Appl. Therm. Eng. 31 (2011) 4014–4023.
[14] J. Bao, L. Zhao, A review of working fluid and expander selections for organic Rankine cycle, Renew. Sustain. Energy Rev. 24 (2013) 325–342.
[15] M. Chys, M. van den Broek, B. Vanslambrouck, M. De Paepe, Potential of zeotropic mixtures as working fluids in organic Rankine cycles, Energy 44 (2012) 623–632.
[16] Q. Liu, Y. Duan, Z. Yang, Effect of condensation temperature glide on the performance of organic Rankine cycles with zeotropic mixture working fluids, Appl. Energy 115 (2014) 394–404.
[17] L. Zhao, J. Bao, Thermodynamic analysis of organic Rankine cycle using zeotropic mixtures, Appl. Energy (2014).
[18] F. Heberle, M. Preißinger, D. Brüggemann, Zeotropic mixtures as working fluids in organic Rankine cycles for low-enthalpy geothermal resources, Renew. Energy 37 (2012) 364–370.
[19] H.J. Chen, D.Y. Goswami, M.M. Rahman, E.K. Stefanakos, A supercritical Rankine cycle using zeotropic mixture working fluids for the conversion of low-grade heat into power, Energy 36 (2011) 549–555.
[20] M. Sadeghi, A. Nemati, A. Ghavimi, M. Yari, Thermodynamic analysis and multi-objective optimization of various ORC (organic Rankine cycle) configurations using zeotropic mixtures, Energy 109 (2016) 791–802.
[21] Y. Wu, Y. Zhu, L. Yu, Thermal and economic performance analysis of zeotropic mixtures for organic Rankine cycles, Appl. Therm. Eng. 96 (2016) 57–63.
[22] L. Zhao, J. Bao, The influence of composition shift on organic Rankine cycle (ORC) with zeotropic mixtures, Energy Convers. Manage. 83 (2014) 203–211.
[23] T. Li, J. Zhu, W. Fu, K. Hu, Experimental comparison of R245fa and R245fa/R601a for organic Rankine cycle using scroll expander, Int. J. Energy Res. 39 (2014) 202–214.
[24] H.C. Jung, L. Taylor, S. Krumdieck, An experimental and modelling study of a 1 kW organic Rankine cycle unit with mixture working fluid, Energy 81 (2015) 601–614.
[25] G.B. Abadi, E. Yun, K.C. Kim, Experimental study of a 1kw organic Rankine cycle with a zeotropic mixture of R245fa/R134a, Energy 93 (2015) 2363–2373.
[26] M. Li, C. Dang, E. Hihara, Flow boiling heat transfer of HFO1234yf and R32 refrigerant mixtures in a smooth horizontal tube: part I. Experimental investigation, Int. J. Heat Mass Transf. 55 (2012) 3437–3446.
[27] E.W. Lemmon, M.L. Huber, M.O. McLinden, NIST standard reference database 23, NIST reference fluid thermodynamic and transport properties–REFPROP, Version 9.0, in: Standard Reference Data Program, National Institute of Standards and Technology, Gaithersburg, MD, 2010.
[28] D. Bivens, A. Yokozeki, Heat Transfer Coefficients and Transport Properties for Alternative Refrigerants, 1994.
[29] S. Zhang S, H. Wang, G. Tao, Performance comparison and parametric optimization of subcritical organic Rankine cycle (ORC) and transcritical power cycle system for low-temperature geothermal power generation, Appl. Energy 88 (2011) 2740–2754.
[30] H. Hettiarachchi, M. Golubovic, W. Worek, Y. Ikegami, Optimum design criteria for an organic Rankine cycle using low-temperature geothermal heat sources, Energy 32 (2007) 1698–1706.